Demonstration of lasercom and spatial tracking with a silicon Geiger-Mode APD array

Timothy M. Yarnall[a], Benjamin W. Horkley[a,b], Ajay S. Garg[a], and Scott A. Hamilton[a]

[a]Massachusetts Institute of Technology, Lincoln Laboratory,
244 Wood St., Lexington, MA 02420;
[b]Massachusetts Institute of Technology, Dept. of Electrical Engineering and Computer Science
77 Mass Ave., Cambridge, MA 02139

ABSTRACT

We present a demonstration of a high-rate photon counting receiver with the potential to act as a spatial tracker based on a silicon Geiger-mode avalanche photodiode array (GM-APD). This array enables sensitive high-rate optical communication in the visible and near infrared regions of the spectrum. The array contains 1024 elements arranged in a 32x32 pixel square. This large number of elements supports high data rates through the mitigation of blocking losses and associated data rate limitations created by the reset time of an individual Geiger-mode detector. Measurement of bit error rates demonstrate that receiver sensitivities of 5.55 dB (detected) photons-per-bit for 78.8 Mb/s on-off-keying and 2.54 dB (detected) photons-per-bit for 19.4 Mb/s 16-ary pulse-position modulation are accessible with strong forward error correction. Additionally, the array can record the spatial coordinates of each detection event. By computing the centroid of the distribution of spatial detections it is possible to determine the angle-of-arrival of the detected photons. These levels of performance imply that Si GM-APD arrays are excellent candidates for a variety of free space lasercom applications ranging from atmospheric communication in the 1 micron or 780 nm spectral windows to underwater communication in the 480 nm to 520 nm spectral window.

Keywords: Photon counting, optical communication, geiger-mode array

1. INTRODUCTION

Photon-counting receivers are well suited to optical communication links that must contend with a great deal of signal loss between transmitter and receiver. In theory, they can provide the best sensitivity in terms of the number of photons required per information bit received allowed by quantum physics in a noiseless channel owing to the Poissonian nature of photon counting.[1] This property makes them especially interesting for deep space[2] and undersea communication links.[3,4] To support high-rate communication a photon-counting receiver must be able to count at high rates, for example, a receiver that only requires 1 photon per bit for error-free operation must be able to register $1 \cdot 10^9$ per second to support a 1 Gb/s link. For a single-element detector this would require a detection and reset time of at most 1 ns; this is largely beyond the capability of semi-conductor based detectors. To circumvent the limitation created by reset time it is possible to split the optical signal over a large number of elements in an array based detector.[5] In this paper, we present the results of photon-counting communication tests based on an arrayed semiconductor photon-counting detector.[6] The array also has the ability to sense the spatial distribution of the received light giving it the potential to act as an optical tracker. We briefly touch on the array's ability to accurately measure the centroid of an incident beam while simultaneous acting as a communication receiver.

Distribution A: Public Release. This work was sponsored by the ASD(R&E) under Air Force Contract #FA8721-05-C-0002. Opinions, interpreta-tions, conclusions, and recommendations are those of the authors and are not necessarily endorsed by the United States Government.

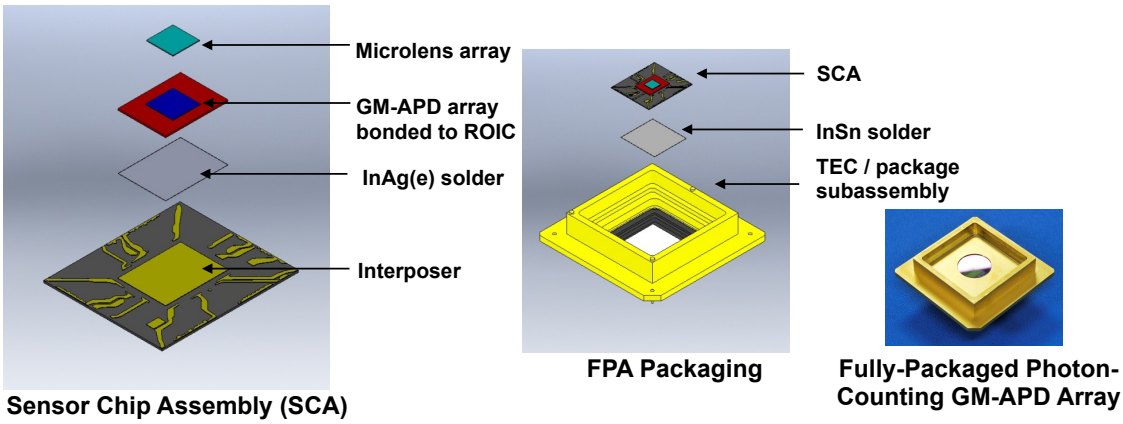

Figure 1: Assembly of GM-APD array with microlens and custom ROIC into a hermetically sealed package with thermo-electric cooling.

2. GEIGER-MODE AVALANCHE PHOTODIODE ARRAY

The key enabling technology for the demonstration reported in this paper is a custom designed Si GM-APD array and readout integrated circuit (ROIC). The array contains 1024 detectors arranged in a 32x32 square. The array active regions are 10 by 10 micron squares spaced on a 100 micron pitch. A microlens array focuses the incoming light onto the active regions of the detector array to mitigate the otherwise low fill factor. The array, microlens, and ROIC are bonded together and sealed in a hermetic package with a thermo-electric cooler, figure 1

One of the unique properties of this detector array is the ROIC. Typically detector arrays operate in one of two modes of operation, a synchronous mode or an asynchronous mode. An array in synchronous operation is armed, read out, and reset in its entirety by a single control circuit; the read out typically includes pixel and time of arrival information. This in advantageous for active imaging applications where the expected return signal will arrive within a known range of times; however, it is undesirable for receiving a communication signal that is continuous in time as the entire array is blocked from registering photons for the duration of the reset time. An array operating asynchronously allows each pixel to reset independently, thus mitigating the blocking issue associated with synchronous operation. The outputs of individual elements in asynchronous arrays are typically passed to an analog summing network thereby erasing any spatial information; this arrangement is referred to as a multi-pixel photon counter. The array used in this work combines the combines the spatial resolution capabilities found in synchronous arrays with the blocking mitigation of asynchronous arrays via a custom ROIC architecture. The ROIC provides a small state-machine to control each pixel in the array. This state machine provides bias for the APD, detects and timestamps incoming photons, actively quenches the APD after an avalanche, and provides a digital read-out that can be processed by higher layers in the ROIC and then transported off-chip digitally. In this way both spatial and temporal information can be recorded continuously making this providing this array with the capability to act simultaneously as a communications receiver and spatial tracker.

3. COMMUNICATION PERFORMANCE

The GM-APD array was evaluated as a photon-counting receiver for high-sensitivity lasercom. As the array used for testing was not a mass-production system, but rather a research-grade prototype, some irregularities were identified that needed to be corrected when using it as a communications receiver. In particular, due to minute differences in the individual detectors, the entire array was not able to be stably operated in Geiger mode at once. An operating voltage of -30.6 V was found to provide the best performance for testing; however, at this voltage, many pixels in the array would be stuck in a state of continuous fire, triggering another fire count immediately after being reset by the ROIC firmware. These always-on pixels, which at times were up to 20%

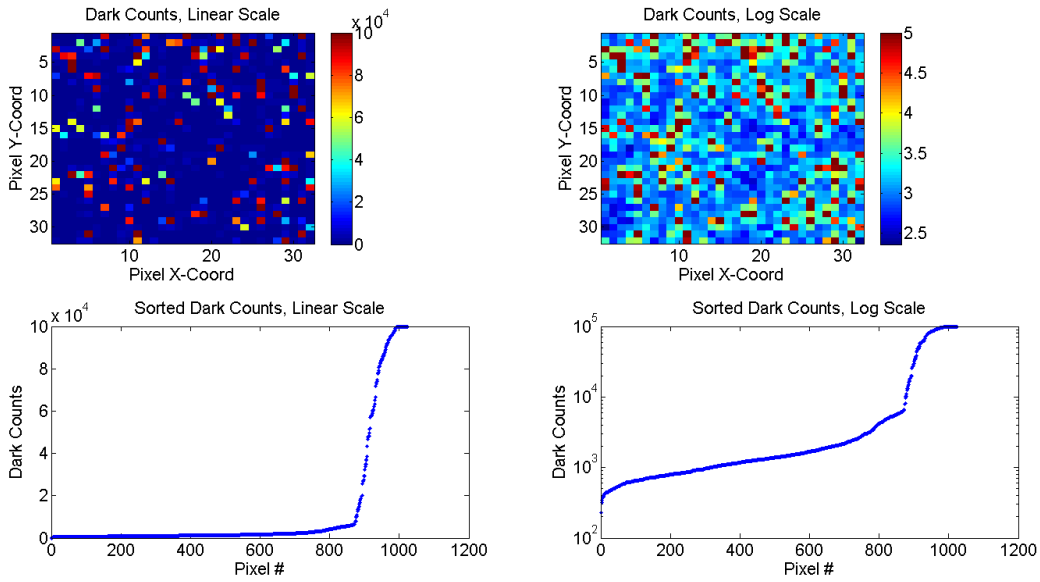

Figure 2: Cumulative distribution of dark counts for a typical unmasked collection. The bottom charts are sorted in ascending order of counts, from the quietest pixel to the noisiest. The spatial distribution of always-on pixels is random, as can be seen in the top grids.

of the array, made a significant negative impact on the sensitivity of the array by increasing the noise floor of the system. Additionally, many of these always-on detectors can create cross-talk via spillover to neighboring detectors. Figure 2 shows a typical distribution of the counts from one of these dark count collections. This level of dark-count noise made communications nearly impossible. Fortunately, this problem can be addressed via the bias voltage management capability of the ROIC, problematic pixels can be deactivated by removing their bias voltage. These issues were dealt with by generating a mask of the most problematic detectors through post-processing a no-light data collection, and then disabling those detectors through the ROIC firmware. A threshold was selected shortly above the "knee" of the distribution, where the number of dark counts began to rise rapidly; in the example distribution shown, this would be at around 5000 counts, out of 80,000 total chances to fire over the capture.

For later tests, a standardized mask was adopted across data collections, to keep the array properties constant while changing data rates and illumination. While initially a new mask was generated for each data set, each of these masks showed little variation from day to day, and the standard was adopted for simplicity and consistency. Rather than the one-level generation described above, this standardized mask was generated in two stages. First, a mask was generated using a higher threshold, which disabled only the most problematic detectors (those which were very close to 100% fire rate). Then, an additional dark count collection was taken using that mask, and a new threshold selected. This two-stage mask generation helped identify detectors which were only problematic as a result of cross-talk and allowed them to be kept active, increasing the array sensitivity. Figure 3 demonstrates the results of this masking; the highest rate of dark counts after masking is about 5% of highest rate pre-masking. A final dark count collection with the array masked was also used to determine the background level for subsequent testing; this is of importance in determining the theoretical performance of the non-ideal array for communications.

The reset time of the ROIC firmware imposes an upper bound on the number of photons the array is able to detect in a given amount of time; if additional photons are incident on a particular APD before it is re-armed, it will simply fail to fire, and the count will not be registered. For low light levels, this is not problematic, as photons are distributed around the array, and the probability of consecutive photons hitting exactly the same detector element is quite low. However, as more photons are incident on the detector, there becomes a higher probability of a detection event being missed because a detector is not reset in time to be re-triggered. The

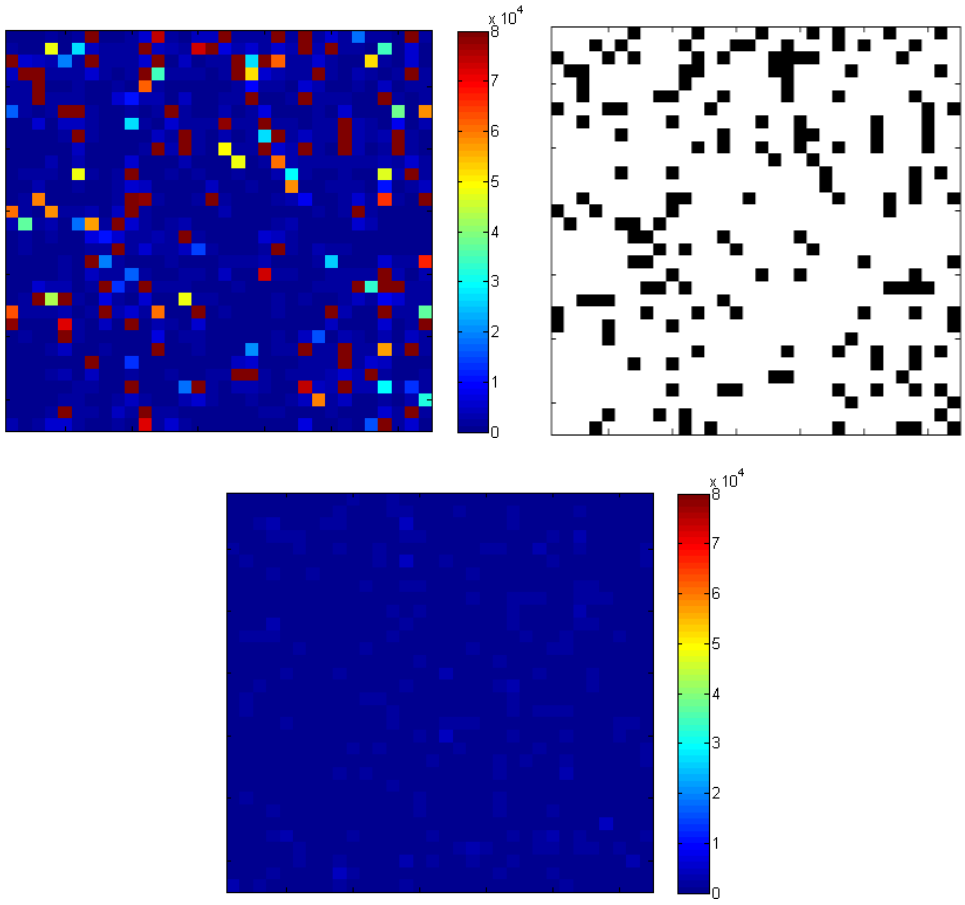

Figure 3: The top left image shows a typical dark count capture, before masking of always-on detectors. The top right image is the standard mask used for communications experiments, with 167 disabled detectors. The bottom image is another dark count capture, with the disable mask applied; the highest dark count rate is about 5% of the rates seen in the unmasked capture.

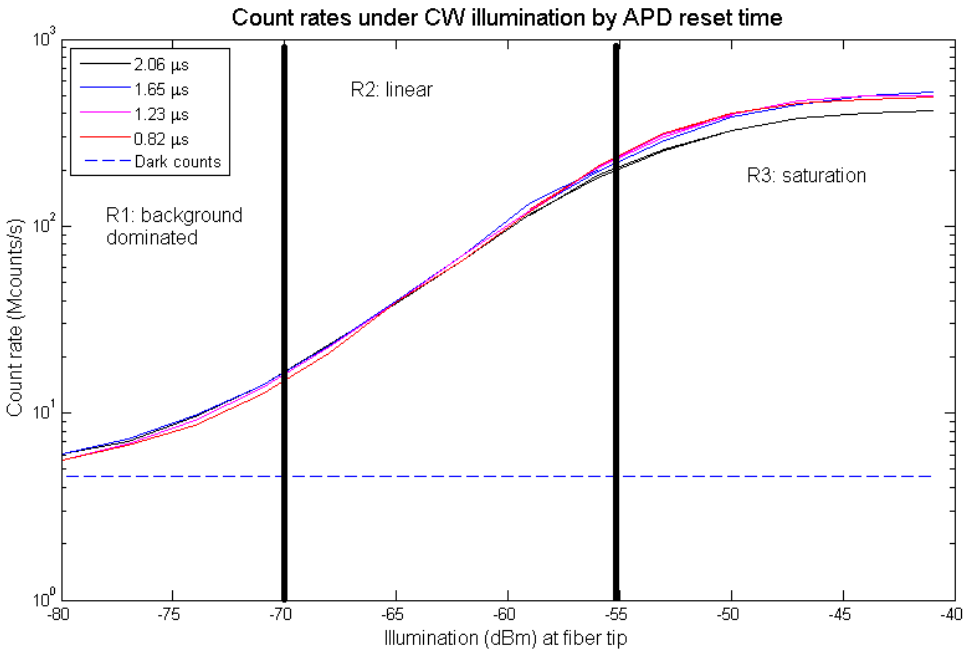

Figure 4: Detected photons vs. input power for several different ROIC minimum reset times: R1, dark count dominated region, R2, linear regime, and R3, saturated regime

maximum counting capacity of the array can be found by simply multiplying the number of active pixels by the maximum rate at which they can be reset and fire again. The minimum inter-arrival time that can be reliably detected on a single array element is programmable to 4 settings 0.82, 1.23, 1.65, and 2.06 μs due to the ROIC design (this limitation could be significantly improved in future designs). With the standardized pixel mask as described in the previous paragraph disabling 167 of the 1024 detectors in the array, this gives an absolute maximum rate of $520 \cdot 10^6$ counts per second. In practice, blocking loss can be observed at input powers significantly below this maximum level because incoming photons are perfectly distributed among all available detectors. This is the case when the array when used as a centroid tracker. Figure 4 shows the rate of counts found under constant illumination at various power levels, with the ROIC firmware's minimum reset time set to several different values.

As indicated in figure 4, the count rates under various illuminations show three broad regions. At low powers, the total count rate is dominated by dark counts, which occur at a rate of roughly 4.5 Mcounts/s over the entire array. At illuminations from about -70 to -55 dBm, the number of detected photons grows roughly linearly with input power. Past that point, around $150 \cdot 10^6$ counts per second, the number of photons the array can detect saturates, approaching the count rate at which all enabled detectors are firing continuously. A maximum count rate of approximately $500 \cdot 10^6$ counts per second, compared to $400 \cdot 10^6$ for the longest reset time. For these reasons, the reset time for all experiments was fixed to be equal to one ROIC frame, 1.65 μs.

Block repeating was also employed to allow the array to operate in the linear regime albeit at a lower data. Block repeating is accomplished by having the transmitter repeat a block of symbols a predetermined number of times, N, so that the receiver can then sum the counts associated with repeated instances of the same symbol. This is analogous to having the transmitter increase the symbol duration by a factor of N or using an array with a factor of N more elements. We chose to use block repeating as it was easier to implement than a variable symbol duration in the transmitter electronics.

3.1 On-OFF Keying (OOK)

The initial communication testing was performed using an RZ (return-to-zero) OOK waveform transmitted at 155 Mb/s in an effort to explore the maximum possible data rate supportable by the array. RZ signaling was

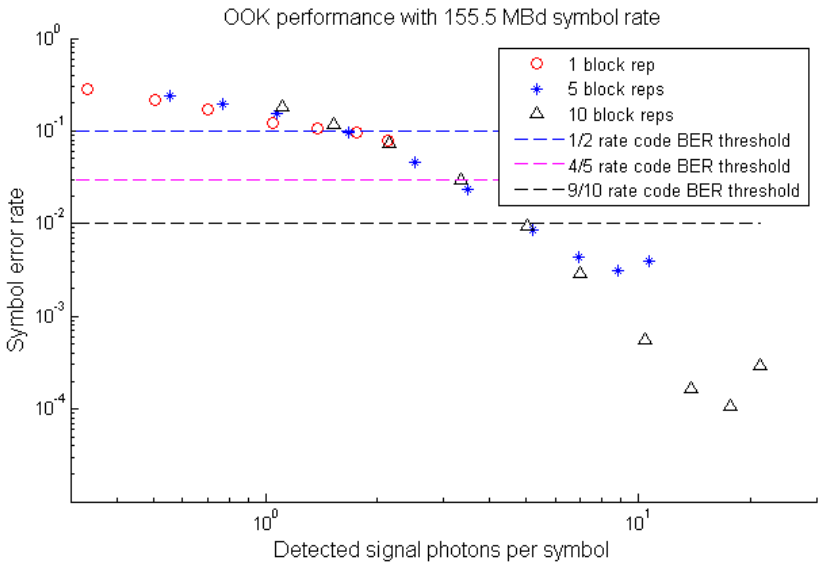

Figure 5: Symbol error rate for OOK modulation at 155.5 MBd.

chosen to assist the receiver in determining symbol boundaries. Figure 5 shows the measured symbol error rate vs counts for $N = \{1, 5, 10\}$ block repeats. The effects of saturation can be scene in the rise of the error rates at the highest input levels recorded with lower error floors observed for 5 and 10 repeats. The thresholds for capacity approaching forward error correction codes are also indicated as horizontal dashed lines. From the intersection of the rate 1/2 threshold with the unrepeated curve at a detection rate of 1.8 counts per symbol implies that error-free operation is possible at 78 Mb/s given 3.6 detections per symbol. Operation with higher rate codes was also considered, but the required block repeating to reach the error thresholds reduced the final information rate to level below what was achievable at rate 1/2 with no block repeats.

3.2 16-ary Pulse Position Modulation (PPM-16)

Communication testing also investigated the performance of PPM-16. This modulation format should be more resilient to blocking losses because the duty cycle of the transmitter is 1/16. In this case the slot rate was also 155 MHz leading to a symbol rate of 9.7 MBaud. Each symbol contains 4 channel bits giving a channel rate of 38.8 Mb/s. Figure 6 shows that by using PPM-16 the receiver could achieve error rates below 10^{-4} without resorting to block repeating. If we again consider the use of a rate-1/2 code with a threshold error rate of 10% we find that error-free operation can be achieved at 19.9 Mb/s given 0.8 detections per channel bit or 1.6 detection per information bit. One can also consider using a rate-4/5 error-correcting code to provide error-free operation at a higher data rate with a small impact on sensitivity. From figure 6 we note that the error curve intersects the threshold for a rate-4/5 code at 1.4 photons per bit. This implies that error-free operation can also be achieved at 31 Mb/s given 1.75 detections per information bit.

4. SPATIAL TRACKING

A GM-APD array such as this one has a great deal of potential for use in a tracking system. The spatial information on the number of fires at each pixel location is available, and the firmware could be modified to process that information in real time, giving a centroid value as an estimate for the beam's position. This centroid information could be fed back to a steering mirror that could adjust the beam such that it centered on the array. One of the challenges in adapting the ROIC firmware for tracking would be in properly accounting for the anomalous always-on pixels. For communications, the only result of deactivating these pixels is a loss of efficiency, as they must be turned off to prevent background noise from overwhelming the detected signal. However, having many detectors turned off, in a random arrangement around the detector array, could have serious consequences

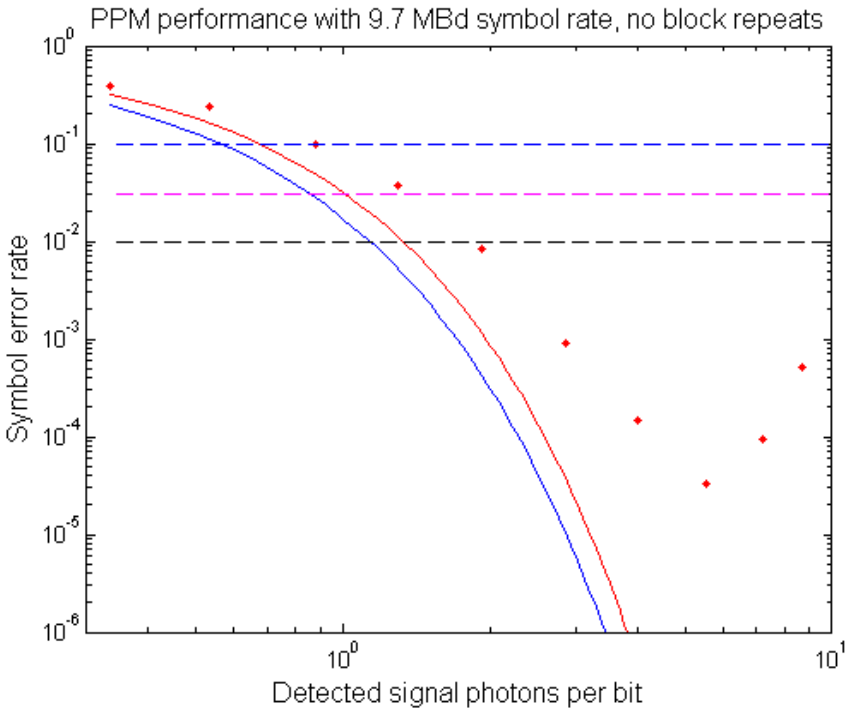

Figure 6: SER for PPM modulation at 9.7 MBd. The blue curve shows the theoretical performance of a detector without dark counts and the red curve shows the expected performance given $4.5 \cdot 10^6$ dark counts per second. From top to bottom, the three dashed lines show the FEC error correction thresholds for rate 1/2, 4/5, and 9/10 codes.

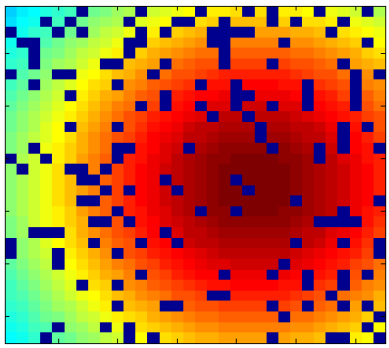

Figure 7: An off-center Gaussian beam illuminating the array when the always-on pixels are deactivated. The error in the computed centroid is 0.4 pixels in the x direction and 1 pixel in the y direction.

for the performance when used for tracking. If the detectors in question are clustered toward a specific part of the array, this can induce a systemic bias into the perceived center of the tracking beam, and feeding back this skewed value to the transmitter would lead to incorrect adjustments. As an extreme example, if the upper right quadrant contained all of the disabled detectors (which for the mask used for communications here would require turning off more than half of the detectors in the quadrant), the perceived center of the tracking beam would be permanently biased toward the lower left quadrant, causing overcorrection in steering the signal toward the part of the array with disabled detectors. Figure 7 shows an example where the mask creates an error in the computed centroid.

One possible scheme to account for this asymmetry would be to create a second mask of detectors in a symmetric pattern about the center that are simply not included in the centroid calculation. While this type of mask could greatly reduce the sensitivity of the array, even halving the number of available detectors should provide the required sensitivity to perform tracking; as many tracking systems currently in use have much more noise than a photon counting sensor. One may also consider interpolating the missing value from neighboring pixels. This approach would have the challenge of adding considerable computation complexity to the firmware, but would preserve the signal information that would be lost in the prior approach. Experimental investigations of these techniques will be the subject of future work.

5. CONCLUSION

This work demonstrates the potential for using a Geiger-mode APD array as both the communications receiver and tracking sensor for a lasercom system. The array is based on silicon technology allowing it to operate over visible wavelengths and in the near infra red making is suitable to support communication in the 1 micron and 780 nm atmospheric windows or the 480 and 520 nm undersea transmission windows. Once mitigations were made for array non-idealities communication performance with the potential for error-free operation were shown for 78.8 Mb/s at 3.6 photons per bit and using OOK modulation and a rate-1/2 code. PPM-16 was also investigated and was shown to support error-free operation for a user rate of 31 Mb/s at 1.8 photons per bit by utilization of a rate-4/5 error-correcting code. Additionally, an initial exploration of the arrays viability as a centroid tracker were made.

ACKNOWLEDGMENTS

The authors would like to thank Brian Aull, Alex McIntosh, and Jonathan Frechette for the development and fabrication and of the GM-APD array as well as many useful discussions for diagnosing and debugging test anomalies as they were encountered.

REFERENCES

1. D. M. Boroson, *Optical communications : A compendium of signal formats, receiver architectures, analysis mathematics, and performance characteristics*, Massachusetts Institute of Technology, Lincoln Laboratory, 2005.
2. D. M. Boroson, B. S. Robinson, D. V. Murphy, D. A. Burianek, F. Khatri, J. M. Kovalik, Z. Sodnik, and D. M. Cornwell, "Overview and results of the lunar laser communication demonstration," *Proc. SPIE* **8971**, pp. 89710S–89710S–11, 2014.
3. H. Hemmati and A. Biswas, "Improving the efficiency of undersea laser communications," *Proc. SPIE* **8971**, pp. 89710I–89710I–7, 2014.
4. P. A. Hiskett and R. A. Lamb, "Underwater optical communications with a single photon-counting system," *Proc. SPIE* **9114**, pp. 91140P–91140P–15, 2014.
5. B. Robinson, D. Caplan, M. Stevens, R. Barron, E. Dauler, and S. Hamilton, "1.5-photons/bit photon-counting optical communications using geiger-mode avalanche photodiodes," *2005 Digest of the LEOS Summer Topicals* , 2003.
6. J. Frechette, P. J. Grossmann, D. E. Busacker, G. J. Jordy, E. K. Duerr, K. A. McIntosh, D. C. Oakley, R. J. Bailey, A. C. Ruff, M. A. Brattain, J. E. Funk, J. G. MacDonald, and S. Verghese, "Readout circuitry for continuous high-rate photon detection with arrays of inp geiger-mode avalanche photodiodes," *Proc. SPIE* **8375**, pp. 83750W–83750W–9, 2012.